FEBS Letters

FEBS PRESS science publishing by scientists

Conversion of an instantaneous activating K^+ channel into a slow activating inward rectifier

Dirk Baumeister[1], Brigitte Hertel[1], Indra Schroeder[1], Sabrina Gazzarrini[2], Stefan M. Kast[3], James L. Van Etten[4], Anna Moroni[2] and Gerhard Thiel[1]

1 Plant Membrane Biophysics, Technical University Darmstadt, Germany
2 Department of Biosciences and CNR IBF-Mi, Università degli Studi di Milano, Italy
3 Physikalische Chemie III, Technische Universität Dortmund, Germany
4 Department of Plant Pathology, Nebraska Center for Virology, University of Nebraska Lincoln, NE, USA

Correspondence
G. Thiel, Plant Membrane Biophysics, Technical University Darmstadt, 64287 Darmstadt, Germany
Fax: +49 6151 16-21942
Tel: +49 6151 16-21940
E-mail: thiel@bio.tu-darmstadt.de

(Received 30 November 2016, revised 14 December 2016, accepted 15 December 2016, available online 2 January 2017)

doi:10.1002/1873-3468.12536

Edited by Maurice Montal

The miniature channel, Kcv, is a structural equivalent of the pore of all K^+ channels. Here, we follow up on a previous observation that a largely voltage-insensitive channel can be converted into a slow activating inward rectifier after extending the outer transmembrane domain by one Ala. This gain of rectification can be rationalized by dynamic salt bridges at the cytosolic entrance to the channel; opening is favored by voltage-sensitive formation of salt bridges and counteracted by their disruption. Such latent voltage sensitivity in the pore could be relevant for the understanding of voltage gating in complex Kv channels.

Keywords: inward rectification; Kcv K^+ channel; salt bridges; voltage-dependent gating

K^+ channels are modular proteins with a central pore and peripheral transmembrane and/or cytosolic domains. The pore domain is responsible for the basic channel functions namely selectivity and gating [1]. It is generally believed that the pore has by itself no genuine voltage dependency. Voltage- and time-dependent gating, which is characteristic of voltage-sensitive K^+ (Kv) channels, is achieved by an electro-mechanical connection between the central pore unit and transmembrane domains (TMD1) in its periphery [2]. The latter consist of four helices (S1–S4), which serve as a voltage sensor domain (VSD). A subset of positively charged amino acids in S4 of these highly conserved sensing domains [3] perceive changes in the transmembrane voltage [4] and transmits them to the pore *via* a short linker [2]. The latter connects the VSD to the pore forming helixes S5 and S6 [5]. In response to depolarization the sensor is moved to the up position, which in turn promotes in outward rectifying channels an opening of the pore gates [4,6,7]. Inward rectifiers become active when S4 moves from the up state to the down state [8,9].

Recent work suggests that the pore unit may by itself generate time- and voltage-dependent gating. Such a latent voltage dependency of the pore was deduced from work with a Kir channel. The introduction of a point mutation in the inner TMD1 of the Kir6.2 pore converted this channel into a slow activating outward rectifier [10]. The mutated channel, which lacks a canonical VSD, exhibits a Kv-type gating and opens upon depolarization in a time- and voltage-dependent manner. Because this voltage-sensitive gating converges with other ligand-operated gates of this channel, it was hypothesized that voltage-dependent gating may be a latent feature of all K^+ channel pores [10]. The same conclusion was reached from work on

Abbreviations
TMD1, transmembrane domain; VSD, voltage sensor domain.

K2P channels. These channels have the general pore architecture of K^+ channels with no canonical voltage sensor. Some members of this channel family nonetheless exhibit a slow activating outward rectification, which is attributed entirely to voltage-dependent gating in the selectivity filter [11]. In much the same vein, single-site mutations within the S6 α-helix of the SKOR K^+ channel convert this outward rectifier into a largely voltage-independent channel, an action that likewise has been ascribed to the characteristics of the selectivity filter [12].

To search for other possible mechanisms of voltage dependency in the pore domain of K^+ channels, we used as a working model the minimal viral K^+ channel Kcv. This channel consists of the pore unit, which is present in all K^+ channels, and lacks large cytosolic domains [13,14]. In spite of its small size (94 aa/monomer) the Kcv channel exhibits distinct voltage dependencies [15,16]. When Kcv is expressed in *Xenopus* oocytes, it responds to a negative voltage by conducting a biphasic current with an instantaneous current and a small superimposed slow activating component. This biphasic kinetics reflects the fact that channels are open at all voltages and that additional channels are activated at moderate voltages in a slow- and voltage-dependent manner [17]. At extreme negative voltages the open channels undergo very short closures. This fast gating can be explained by a gating in the filter [15]; it is the cause of a negative slope conductance of the I/V relation at extreme negative voltages.

The aforementioned slow activation of channels at negative voltages is lost in mammalian cells when the channel is expressed as a fusion protein with GFP [18]. These experimental results support the hypothesis of a latent voltage dependency in K^+ channel pores, which may be present or disappear following minor changes in the protein or in the lipid environment in which the protein functions. This view is further supported by experiments in which the slow time- and voltage-dependent gating of the channel was recovered in mammalian cells after insertion of a single Ala into the outer TMD1 of the Kcv channel [19]. This mutant exhibits features of a Kv-type inward rectifier; it closes at positive voltages and activates in a time-dependent manner at negative voltages. Here, we examine the voltage dependency of this synthetic inward rectifier and analyze the underlying gating mechanism. The data support a model, in which the formation and disruption of salt bridges [19] at the cytosolic entry in combination with the transported ion forms a gate. The voltage dependency and the slow dynamics of channel gating could therefore be caused by a voltage sensitivity in the formation of salt bridges.

Materials and methods

The Kcv channel or its mutants were transiently expressed as chimeras with a C-terminally linked GFP as reported previously [19]. Currents were measured as in [19] at different temperatures in a standard medium containing 100 mM KCl, 1.8 mM $CaCl_2$, 1 mM $MgCl_2$, and 5 mM HEPES (pH 7.4); mannitol was used to adjust the osmolarity to 300 mOsmol. The temperature was changed by cooling or heating the perfusion buffer. The actual bath temperature during a recording was monitored by a microthermometer (GTH1200 digital-thermometer; Greisner Electronics, Regenstauf, Germany). The pipettes contained 130 mM D-potassium-gluconic acid, 10 mM NaCl, 5 mM HEPES, 0.1 mM GTP (Na salt), 0.1 μM $CaCl_2$, 2 mM $MgCl_2$, 5 mM phosphocreatine, 2 mM ATP (Na salt; pH 7.4). Currents were measured in a whole-cell configuration by clamping cells from holding voltage (0 mV) to testing voltages between +60 and −160 mV.

Yeast complementation experiments were done with the yeast strain SGY1528 (Mat *a ade* 2–1 *can* 1–100 *his* 3–11,15 *leu* 2–3,112 *trp* 1–1 *ura* 3–1 *trk* 1::HIS3 *trk* 2::TRP1) as described previously [20].

Images of GFP-tagged Kcv in HEK293 cells were acquired with a Leica SP confocal system (Leica Microsystems, Wetzlar, Germany) equipped with a 63× Apo plan water objective. GFP fluorescence was excited by a 488-nm laser line and detected in the range from 505 to 540 nm.

Results

The expression of the Kcv::GFP channel in HEK293 cells reveals a conductance, which is moderately inward rectifying; steps to positive and negative voltages elicit in this system instantaneous activating inward and outward currents with no apparent time dependency. Typical examples of a mock transfected HEK293 cell and of a Kcv::GFP-expressing cell [18] are shown in Fig. 1B,C, respectively. It was previously shown that the channel gains a slow activating kinetics at negative voltages, when TMD1 was elongated by one Ala at position 16 [19].

The data in Fig. 1D show that the current acquired the same pronounced biphasic activation when TMD1 was extended by one Ala, at position 17 (Kcv::GFP-A17). Negative voltages elicited in this case a slow activating inward conductance, which was superimposed on an instantaneous activating current; the slow component contributed 49 ± 8% to the total current at −140 mV. This current slowly decreased at positive voltages and increased at negative voltages (Fig. 1D, E). Altogether, the complex kinetics produced a pronounced inward rectification of the steady state I/V relation (Fig. 1F inset).

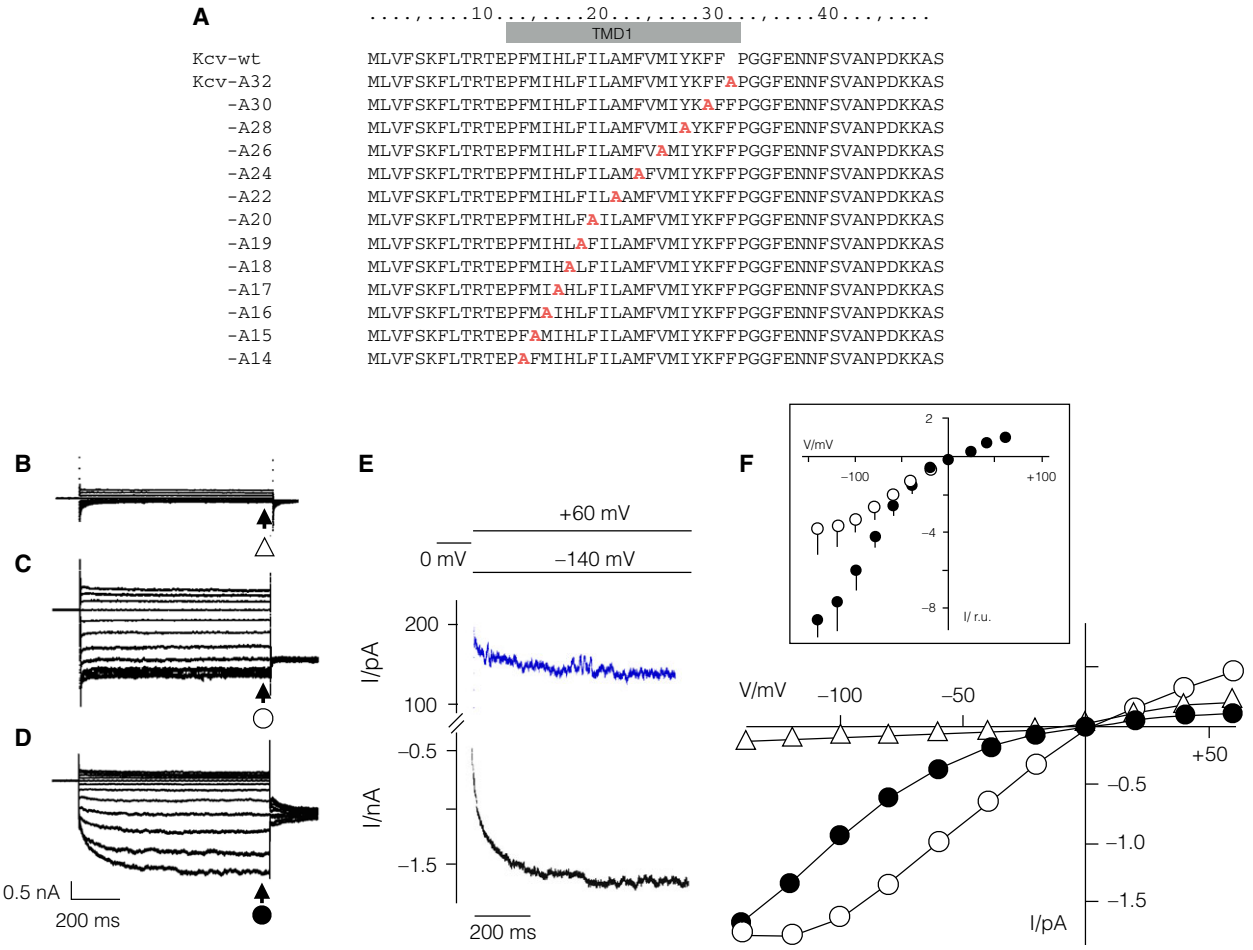

Fig. 1. (A) Sequence of the N terminus of Kcv::GFP channel (Kcv::GFP-wt) with location (gray bar) of the outer transmembrane domain (TMD1). The rows below the wt sequence indicate the position in which an Ala was inserted (red). Current responses of HEK293 cells expressing only GFP (B), Kcv::GFP-wt channel (C) or Kcv::GFP-A17 mutant (D). (E) Magnification of current responses from (D) to voltage steps to +60 mV (blue) and −140 mV (black). The steady-state currents in (B–D) were collected at the end of the voltage pulse (indicated by arrows) and were plotted in (F). Inset: mean *I*/*V* relation (±SE of $n \geq 10$) of Kcv::GFP-wt channel and Kcv::GFP-A17 mutant normalized to current at +60 mV. Symbols in (F) correspond to those in (B–D).

Inspired by this finding we inserted a single Ala in different positions along the outer TMD1 of Kcv (Fig. 1A) and monitored the resulting currents in HEK293 cells. We found that a slow activating inward conductance was also observed after inserting an Ala in positions 14–16 in TMD1 (Figs 1A and 2A). In all cases negative voltages elicited in these mutants the slow activating inward current superimposed on an instantaneous activating current (Figs 2A and 3A, Fig. S1). Only when the Ala was inserted downstream of position 17, the resulting currents were no longer distinguishable from those of nontransfected cells (Fig. 2A,B). To investigate the lack of current in constructs Kcv::GFP-A18 to A32 we examined fluorescent images of HEK293 cells expressing these channel constructs. An example is shown for HEK293 cells, which transiently express Kcv::GFP-A22. These cells show the same distribution of the fluorescence as those expressing the wt channel (Fig. S2). The results of these experiments suggest that an insertion of an Ala in the upper part of TMD1 does not interfere with channel synthesis, assembly and/or trafficking. The insertion apparently renders these channels inactive.

The same sharp transition between active and inactive Kcv channels was confirmed in yeast complementation assays (Fig. 2C). In this case, yeast mutants that lack their own K^+ uptake system were transfected with Kcv-wt and mutants in which an Ala was inserted between positions 16 and 19 into TMD1. The data

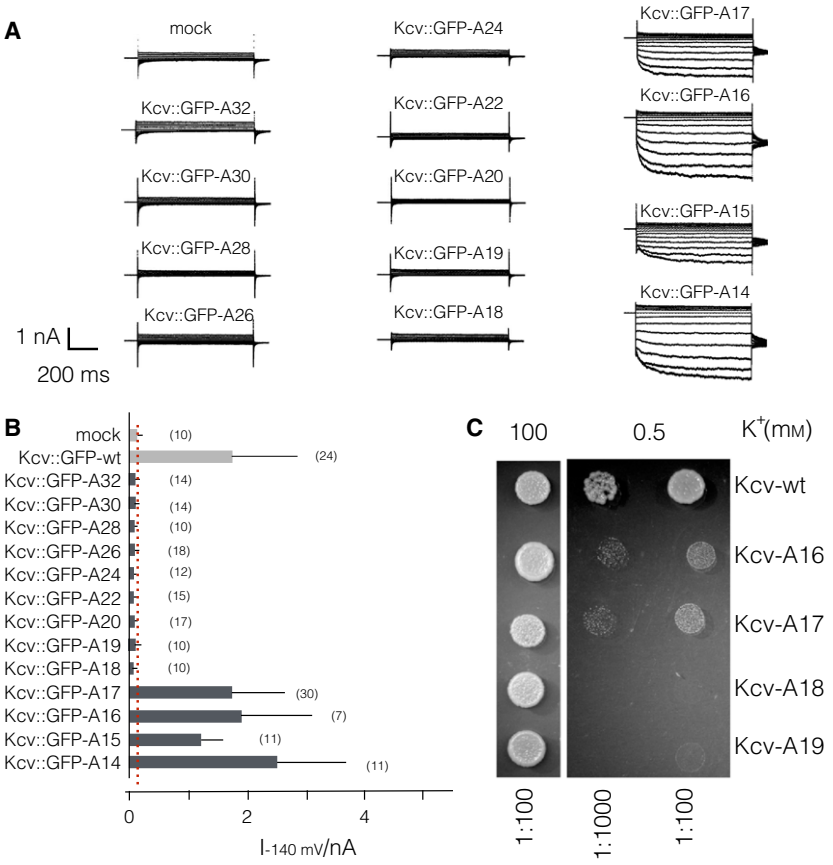

Fig. 2. Current responses of HEK293 cells expressing different constructs in which an Ala was inserted in TMD1 (A). The mean steady-state currents (±SD) evoked by clamp step to −140 mV in measurements as in (A) are shown in (B) for wt channel, mutants as well as for mock transfected cells. The number of recordings is shown in brackets. The red line marks the mean current recorded in mock transfected cells. (C) Complementation of growth of yeast mutants by expression of Kcv::GFP-wt and mutant channels with Ala insertions at different positions. All yeasts grow on nonselective medium with 100 mM K^+. Under selective conditions with 0.5 mM K^+ only the Kcv::GFP-wt channel as well as Kcv::GFP-A16 and A17 are able to rescue growth. Yeast mutants, which express Kcv::GFP-A18 and A19 did not grow in low K^+ medium.

show that the mutants, Kcv-A16 and A17 complemented yeast growth indicating that these channels were active. The mutants Kcv-A18 and A19, which failed to rescue the yeast, also did not generate a current in HEK293 cells (Fig. 2A,B). These experimental results confirm that Ala insertion in the top half of the TMD1 results in nonfunctional channels.

The slow activating inward rectification, which appeared in mutants that tolerated the Ala insertion, is typical for Kv-type voltage-dependent inward rectifiers [21,22]. This is an interesting observation considering the pore-only nature of Kcv and the absence of any VSD in this channel. To quantify the voltage dependency of the slow activating mutants we obtained activation curves from tail currents. Figure 3A shows an example of the tail currents from mutant Kcv::GFP-A17. A HEK293 cell expressing this mutant was clamped from a holding voltage of 0 mV to test voltages between +60 mV and −140 mV and finally to a common post voltage at −80 mV. The tail current at −80 mV was collected 5 ms after the voltage step and plotted as a function of the conditioning voltage. The corresponding activation curve (Fig. 4B) can be fitted by a Boltzmann function in the form

$$I = (I_{max} - I_{vi})/(1 + \exp(zF(V_{1/2} - V)/RT)) + I_{vi} \quad (1)$$

where I_{max} denotes the maximal current, z the gating charge, $V_{1/2}$ the voltage for half maximal current activation and I_{vi} the fraction of voltage-independent currents. R, T, and F have their usual thermodynamic meanings. In the present case, a fit yielded a value of −75 mV for $V_{1/2}$, a 0.83 for z and an I_{vi} of −383 pA (Fig. 3B). The same analysis was performed with the other three constructs (A14–16), which generated a slow inward rectification (Fig. 3C). The fitting results show that insertion of Ala in all four positions in TMD1 elicited the same parameters $V_{1/2}$ and z of the A17 construct. Altogether this suggests that any extension of TMD1 in the critical region converts the channel into the same type of inward rectifier. The average voltage dependency of these channels has a value of $z = 0.8 \pm 0.15$. This means that the responsible 'voltage sensor' feels nearly the entire electrical field. For comparison, a canonical Kv-type inward rectifier like KAT1 has a z value of 1.4 [23]. Hence, the presence of an S4 domain only increases the voltage sensitivity by a factor of two.

To estimate the energy barrier for the slow voltage-dependent gate we recorded the currents of the

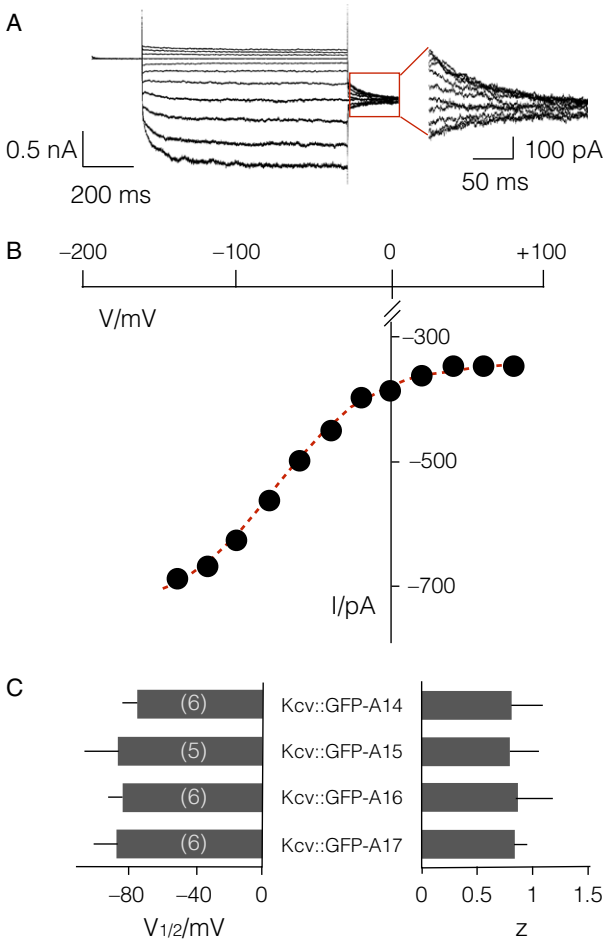

Fig. 3. Activation curve of Kcv::GFP-A17 mutant. (A) Activation of current by voltage steps from +60 to −140 mV and current relaxation of tail currents by stepping membrane voltage to −80 mV. Tail currents from red box, are magnified on the right. (B) Plot of initial tail currents as a function of the conditioning voltage. The data were fitted by a Boltzmann function (Eqn 1) yielding a value of −75 mV for $V_{1/2}$ and a value of 0.83 for z. (C) Mean values ± SD for $V_{1/2}$ and z for the same analysis of indicated mutants. The number of cells analyzed is indicated in brackets.

Kcv::GFP-A17 mutant at temperatures between 11 °C and 37 °C [24]. Typical results for the kinetics of the slow current from one cell at five different temperatures are reported in Fig. 4A. The data indicate that slow activation was accelerated by increasing temperatures. To quantify the process, the activation kinetics was fitted by exponential equations; a single exponential was sufficient to describe the kinetics of slow current activation (Fig. 4A inset). The temperature dependence of the activation kinetics was analyzed by an Arrhenius plot (Fig. 4B) showing a linear relationship for current activation recorded in response to clamp steps from 0 mV to test voltages between −80 mV and −140 mV. Line fits of the data sets provide a value for the energy barrier for activation of 26 ± 3 $kJ \cdot mol^{-1}$ at −80 mV, 36 ± 4 at −100 mV, 39 ± 4 at −120 mV, and 41 ± 2 $kJ \cdot mol^{-1}$ and −140 mV and logarithmic pre-exponential factors (normalized to a standard time unit of seconds) of 13.4 ± 1.2, 18.1 ± 1.0, 22.9 ± 0.8, and 20.1 ± 0.7 at the respective voltages. The differences in the energy barrier between the 4 V furthermore indicates that the energy barrier increased with increasing negative voltage (Fig. 4C). If we assumed as an approximation for the slow gating process a two-state system involving forward and backward reactions only, then the formal Arrhenius activation energies would be essentially given by the faster component (lower activation energy) only, since the overall kinetic time constant were under these circumstances given by the sum of two individual, forward and backward, contributions. The presence of biphasic current kinetics with an instantaneous and a slow current component, however, indicates a more complicated kinetic scheme. As elaborated further in the discussion below, we view the slow kinetics as a distinct two-state system, which allows us to draw qualitative conclusions about the microscopic origin of the observed behavior.

An additional observation was that the slow kinetic component of the current tends to disappear upon cooling; this is apparent in the trace recorded at 11 °C (Fig. 4A). From this behavior, we speculated that the Kcv::GFP-wt channel may fail to exhibit a slow current component in HEK293 cells because of a different energy barrier. To test this hypothesis we recorded the currents of Kcv::GFP-wt in HEK293 cells at 21 °C and at 40 ± 2.5 °C. Figure 5 illustrates typical current responses of the same HEK293 cell to a voltage step from 0 to −140 mV at the two temperatures. The data show that the current at 21 °C responds instantaneously to the negative voltage step; it has no apparent time-dependent component. The same voltage step elicited a smaller instantaneous current at a higher temperature, which then slowly increased toward the steady-state current measured at room temperature (Fig. 5). Similar results were obtained in three other experiments, which showed that an increase in temperature decreased the amplitude of the instantaneous activating current. The current then increased slowly toward the steady-state current, which was measured at low temperature.

Discussion

The main result of our study is that an ion channel, which consists of nothing more than the canonical pore module of K^+ channels [13,14,25], can be

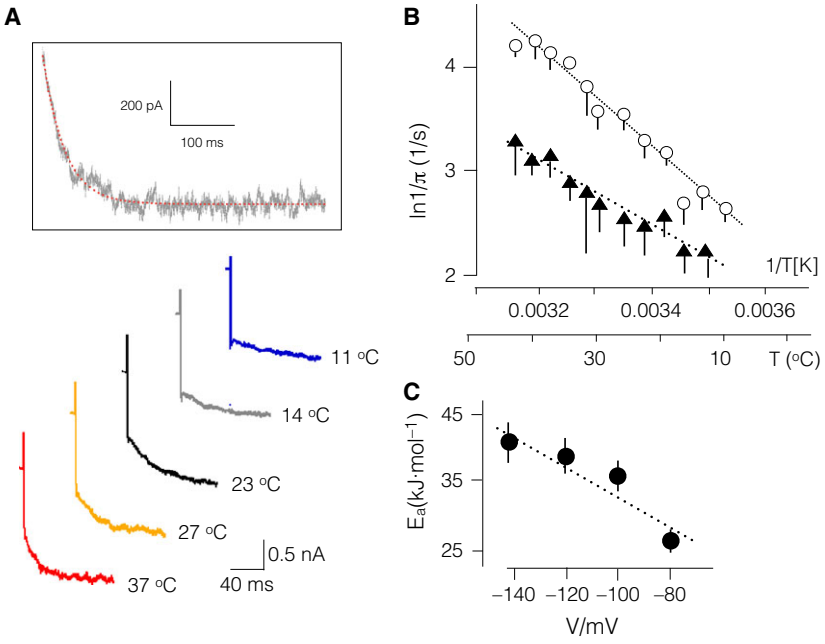

Fig. 4. Temperature dependency of slow current activation in Kcv::GFP-17A mutant. (A) Examples of current responses to voltage steps from 0 to −140 mV from one HEK293 cell expressing Kcv::GFP-17A mutant at different temperatures, which are given as numbers along traces. The slow component of the current response was fitted by a single exponential (inset), the effective time constant of which corresponds to the sum of opening and closing constants. (B) Arrhenius plots for the slow kinetic component elicited by a test pulse to −140 (open circles) and −80 mV (triangles). The effective energy of activation (E_a) obtained from the slopes = $-E_a/R$ (dotted lines) is shown in (C) as a function of the clamp voltage.

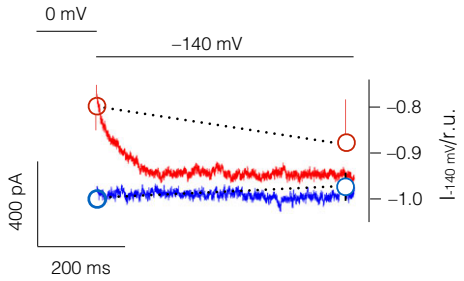

Fig. 5. Temperature induced kinetics of Kcv::GFP-wt current. Current responses of one HEK293 cell expressing Kcv::GFP-wt to voltage step from 0 mV to −140 mV at room temperature (21 °C, blue line) and at 40.2 ± 2.5 °C (red line). The open circles show normalized mean currents (±SD) at the same voltage step from measurements in four cells for the instantaneous current and for the steady-state current. Data were normalized to instantaneous current measured at room temperature (22.5 ± 0.9 °C).

converted from an instantaneous to a slow activating inward rectifier by the insertion of a single Ala into TMD1. This supports the view that K^+ channel pores have a latent voltage dependency [10,11]. Small changes, like single amino acid exchanges [10] or, as in the present case, an insertion of an amino acid, are sufficient to convert a channel with no apparent voltage sensitivity into a voltage-sensitive channel with slow activation kinetics. It is reasonable to speculate that these mutations produce changes in Kcv, which might also occur in other, more complex channels, such as for instance the voltage-gated K^+ channels. In other words, it is possible that an inherent voltage sensitivity of the channel pore could contribute to the voltage sensitivity in Kv channels.

These results point to local interactions between the cluster site within the S6 transmembrane helix and the base of the pore helix as a key element in coupling K^+ and V sensitivity and gating, and they imply a role for cation occupancy of the channel pore in this process.

Previous computational data have highlighted a strong mechanical interaction between the short N terminus and the C terminus of the channel [26]. From molecular dynamic simulations and experimental validations, it occurred that positively charged amino acids (K6 and R10) on the N-terminal helix of the Kcv channel form salt bridges with the negatively charged C-terminus [14,25,27]. In this context, we have previously demonstrated that salt bridges are important for gating and that Kcv is conductive only in their presence because they remove the negatively charged C terminus out of the conducting pathway as they compete for binding of the C terminus with the permeant cation. A channel is only conductive when the salt bridges can form. In their absence, the negatively charged C terminus strongly interacts with a positively charged K^+ ion thus trapping the channel in a nonconductive state ([14,27] Fig. 6). The present data can be explained in the context of a modulation of salt bridge dynamics. The negative charge of the very C terminus of Kcv is, in the case of Kcv::GFP, substituted by the presence of an anionic amino acid in the linker that connects Kcv to GFP (Fig. S3). The insertion of an additional Ala in TMD1 causes a rotation plus a dislocation of the

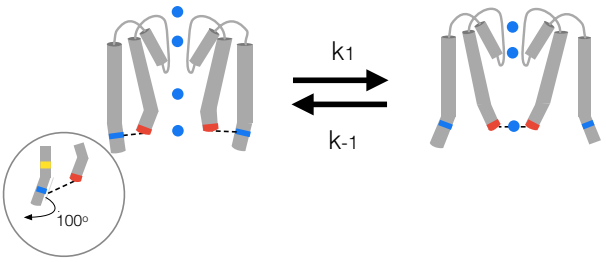

Fig. 6. Proposed model to explain the slow gating. The negative C terminus of the channel (red) can either complex a K^+ ion (blue sphere) or form a salt bridge (dotted line) with cationic amino acids (blue square) in the short N-terminal cytosolic domain of the channel. Salt bridge formation opens the channel (left) and interaction of the C terminus with K^+ ions interrupts ionic current (right). In the chimera with GFP the role of the negative carboxyl terminus is taken over by an anionic amino acid in the linker between channel and GFP. Inset: Insertion of an Ala (yellow bar) upstream of Pro13 (kink), which forms the onset of TMD1, displaces the N terminus downward and turns it by 100°.

N-terminal helix with respect to the C terminus of the channel (Fig. 6). This displacement of the N-terminal helix has a negative impact on the stability of the critical salt bridges in this part of the channel and hence favors channel closing.

Given the importance of salt bridges for channel function, we suggest a simple model to explain the slow gating in the Ala insertion mutant (Fig. 6). The activity of the channel is determined by forming (k_1) and disrupting (k_{-1}) salt bridges at the cytosolic entrance; channel opening is augmented by their formation and counteracted by their disruption [14,25]. Since the open probability for this channel is low (below 5%, [15]), we generally have $k_1 \ll k_{-1}$. In this case, the formal 'effective' Arrhenius activation energy (as analyzed according to Fig. 4) is given by

$$E_{a,\mathrm{eff}} = \frac{k_1 E_{a,1} + k_{-1} E_{a,-1}}{k_1 + k_{-1}} \approx E_{a,-1} \qquad (2)$$

that is, corresponding essentially to the closing process. We can therefore hypothesize that the rate with which the channel state switches is determined by the kinetics related to the breaking of the salt bridges. This view is supported by the experimental data as an effective activation energy on the order of 26–40 $kJ{\cdot}mol^{-1}$ was revealed by the Arrhenius plot in Fig. 4B. This value is close to 30 $kJ{\cdot}mol^{-1}$, which is required to break salt bridges in the tertiary and quaternary structure of proteins [28]. The fact that this activation energy increases with hyperpolarizing voltages (Fig. 4C) implies that the underlying process, for example, the opening of salt bridges becomes more difficult at negative voltages. The electrical field presumably stabilizes the salt bridge interactions indirectly by increasing the barrier height, near which the distance between salt bridge partners must be increased compared to the bound state. The transition state becomes more solvent-separated 'ion pair'-like compared to the compact dipole formed within the bridge, and therefore more susceptible to the effect of an external field. Indeed, it has been shown that the hydration free energy of an ion increases with larger field strength [29] and it can be expected that this effect is less pronounced for dipole–solvent interactions. Ultimately, molecular simulations will be necessary to elucidate the detailed microscopic origin.

A further indication of the relevance of salt bridge dynamics for the observed kinetics is provided by analysis of the Arrhenius prefactors, which can be interpreted as an effective upper limit for the 'attempt' frequencies to pass a barrier. Ignoring the somewhat outlying data at −80 mV, which suffers from severe noise, the average yields around $7.5 \times 10^7\ s^{-1}$. This value lies within an order of magnitude in the range of experimentally observed infrared-spectral signature of salt bridge flips. The latter are found around 2200 cm^{-1}, corresponding to a characteristic frequency of $1.4 \times 10^7\ s^{-1}$ [30].

The interpretation of gating on the basis of salt bridge dynamics is interesting in the context of the voltage dependency of the channel pore. Kcv has no obvious voltage sensor; the TMD1s contain only two cationic amino acids, which are in the electrical field (Fig. S3). Since one of them, K29, was already neutralized without any effect on channel gating [20], the present data suggest that other structures must serve as a voltage sensor. One possibility is that the salt bridges themselves are part of voltage sensing. The closed salt bridge will form a dipole, which is at the edge of the electrical field. This dipole may sense a sufficient fraction of the electrical field for destabilizing the salt bridges and hence closing the channel at positive voltage. An even larger impact will have the free charges of the open salt bridges in sensing voltage. From the present results we are not able to judge if the salt bridges are able to sense enough of the electrical field to explain the steep voltage dependency of gating. As an alternative it is also possible that the selectivity filter is, like in K2P channels [11], responsible for the voltage dependency. The filter, which presumably experiences the largest voltage drop, could be coupled *via* long-range interactions with the gate at the cytosolic entry; such a coupling has been proposed for the gating of the KcsA channel [31]. Further kinetic analysis will be necessary to shed more light on the microscopic details.

Acknowledgements

This research was supported by the LOEWE initiative iNAPO (GT), the Deutsche Forschungsgemeinschaft SCHR1467/1-1 (IS), PGR00139 from MAECI (Ministero Affari Esteri e Cooperazione Internazionale), CARIPLO grant 2014-0660 (AM) and grant 2014-0728 to DD. NSF – EPSCOR Grant EPS-1004094 (JVE) and the COBRE program of the National Center for Research Resources Grant P20-RR15535 (JVE).

Author contributions

DB, BH and SG performed experiments, DB, IS and GT analyzed data. AM, SK and GT planned study, AM, JV, SK and GT wrote paper.

References

1 Kim DM and Nimigean CM (2016) Voltage gated potassium channels: a structutural examination of selectivity and gating. *Cold Spring Harb Perspect Biol* **8**, 1–20.
2 Blunck R and Batulan Z (2012) Mechanism of electromechanical coupling in voltage-gated potassium channels. *Front Pharmacol* **3**, 1–16.
3 Palovcak E, Delemotte L, Klein ML and Carnevale V (2014) Evolutionary imprint of activation: the design principles of VSDa. *J Gen Physiol* **143**, 145–156.
4 Bezanilla F (2000) The voltage sensor in voltage-dependent ion channels. *Physiol Rev* **80**, 555–592.
5 Long SB, Campbell EB and MacKinnon R (2005) Voltage sensor of Kv1.2: structural basis of electromechanical coupling. *Science* **309**, 903–908.
6 Gandhi CS and Isacoff EY (2002) Molecular models of voltage sensing. *J Gen Physiol* **120**, 455–463.
7 Horn R (2002) Coupled movements in voltage-gated ion channels. *J Gen Physiol* **120**, 449–453.
8 Latorre R, Olcese R, Basso C, Gonzalez C, Munoz F, Cosmelli D and Alvarez O (2003) Molecular coupling between voltage sensor and pore opening in the *Arabidopsis* inward rectifier K^+ channel KAT1. *J Gen Physiol* **122**, 459–469.
9 Männikkö R, Elinder F and Larsson HP (2002) Voltage-sensing mechanism is conserved among ion channels gated by opposite voltages. *Nature* **419**, 837–841.
10 Kurata H, Rapedius M, Kleinman MJ, Baukrowitz T and Nichols CG (2010) Voltage dependent gating in a voltage sensor-less" ion channel. *PLoS Biol* **8**, e1000315.
11 Schewe M, Nematian-Ardestani E, Sun H, Musinszki M, Cordeiro S, Bucci G, de Groot BL, Tucker SJ, Rapediua M and Baukrowitz T (2016) A non-canonical voltage-sensing mechanism controls gating in K2P K^+ channels. *Cell* **164**, 937–949.
12 Johansson I, Wulfetange K, Porée F, Michard E, Gajdanowict P, Lacomb B, Sentenac H, Thibaud JB, Mueller-Roeber B, Blatt MR, *et al*. (2006) External K^+ modulates the activity of the *Arabidopsis* potassium channel SKOR via an unusual mechanism. *Plant J* **46**, 269–281.
13 Plugge B, Gazzarrini S, Nelson M, Cerana R, Van Etten JL, Derst C, DiFrancesco D, Moroni A and Thiel G (2000) A potassium channel protein encoded by chlorella virus PBCV-1. *Science* **287**, 1641–1644.
14 Tayefeh S, Kloss T, Kreim M, Gebhardt M, Baumeister D, Hertel B, Richter C, Schwalbe H, Moroni A, Thiel G *et al*. (2009) Model development for the viral Kcv potassium channel. *Biophys J* **96**, 485–498.
15 Abenavoli A, DiFrancesco M, Schroeder I, Epimashko S, Gazzarrini S, Hansen UP, Thiel G and Moroni A (2009) Fast and slow gating are inherent properties of the K^+ channel pore module. *J Gen Physiol* **134**, 869–877.
16 Gazzarrini S, Van Etten JL, DiFrancesco D, Thiel G and Moroni A (2002) Voltage-dependence of virus encoded miniature K^+-channel Kcv. *J Membr Biol* **187**, 15–25.
17 Gazzarrini S, Abenavoli A, Gradmann D, Thiel G and Moroni A (2007) Electrokinetics of miniature K^+ channel: open state V-sensitivity and inhibition by K^+ driving force. *J Membr Biol* **214**, 9–17.
18 Moroni A, Viscomi C, Sangiorgio V, Pagliuca C, Meckel T, Horvath F, Gazzarrini S, Valbuzzi P, Van Etten JL, DiFrancesco D *et al*. (2002) The short N-terminus is required for functional expression of the virus encoded miniature K^+-channel Kcv. *FEBS Lett* **530**, 65–69.
19 Hertel B, Tayefeh S, Mehmel M, Kast SM, Van Etten JL, Moroni A and Thiel G (2006) Elongation of outer transmembrane domain alters function of miniature K^+ channel Kcv. *J Membr Biol* **210**, 21–29.
20 Gebhardt M, Hoffgaard F, Hamacher K, Kast SM, Moroni A and Thiel G (2011) Membrane anchoring and interaction between transmembrane domains is crucial for K^+ channel function. *J Biol Chem* **286**, 11299–11306.
21 Lai H, Grabe M, Jan YN and Jan LY (2005) The S4 voltage sensor packs against the pore domain in the KAT1 voltage-gated potassium channel. *Neuron* **47**, 395–406.
22 Lefoulon C, Karnik R, Honsbein A, Vijay Gutla P, Grefen C, Riedelsberger J, Poblete T, Dreyer I, Gonzalez W and Blatt MR (2014) Voltage-sensor transitions of the inward-rectifying K^+ channel KAT1 indicate a latching mechanism biased by hydration within the voltage sensor. *Plant Physiol* **166**, 960–975.
23 Hertel B, Horvath F, Wodala B, Hurst A, Moroni A and Thiel G (2005) KAT1 inactivates at sub-millimolar

concentrations of external potassium. *J Exp Bot* **422**, 3103–3110.
24 Rodriguez BM, Sigg D and Bezanilla F (1998) Voltage gating of Shaker K^+ channels: the effect of temperature on ionic and gating currents. *J Gen Physiol* **112**, 223–242.
25 Tayefeh S, Kloss T, Thiel G, Hertel B, Moroni A and Kast SM (2007) Molecular dynamics simulation of the cytosolic mouth in Kcv-type potassium channels. *Biochemistry* **46**, 4826–4839.
26 Hoffgaard F, Kast SM, Moroni A, Thiel G and Hamacher K (2015) Tectonics of a K^+ channel: the importance of the N-terminus for channel gating. *Biochim Biophys Acta* **1848**, 3197–3204.
27 Hertel B, Tayefeh S, Kloss T, Hewing J, Gebhardt M, Baumeister D, Moroni A, Thiel G and Kast SM (2009) Salt bridges in the miniature viral channel Kcv are important for function. *Eur Biophys J* **39**, 1057–1068.
28 Gruia AD, Fischer S and Smith JC (2004) Kinetics of breaking a salt-bridge critical in protein unfolding. *Chem Phys Lett* **385**, 337–340.
29 Gavryushov S and Linse P (2003) Polarization deficient and excess free energy of ion hydration in electrical fields. *J Phys Chem B* **107**, 7135–7142.
30 Vener MV, Odinokov AV, Wehmeyer C and Sebastiani D (2015) The structure and IR signature of arginine-glutamate salt bridge. Insights from the classical MD simulation. *J Chem Phys* **142**, 215106.
31 Hulse RE, Sachleben JR, Wen PC, Moradi M, Tajkjorshid E and Perozo E (2014) Conformational dynamics at the inner gate of KcsA during activation. *Biochemistry* **53**, 2557–2559.

Supporting information

Additional Supporting Information may be found online in the supporting information tab for this article:
Fig. S1. I/V curves of Kcv::GFP-wt channel and mutants with Ala insertions.
Fig. S2. Confocal images of HEK293 cells expressing GFP-tagged Kcv::GFP-wt channel (left) and Kcv::GFP-A22 mutant (right).
Fig. S3. Amino acid sequence Kcv::GFP highlighting cationic (red) and anionic (blue) amino acids outside and inside (gray bars) of transmembrane domains of the channel.